10.3217/978-3-99161-014-4-005

RECOGNITION OF PERTURBATION EVOKED POTENTIAL BY USING MIXED-DEPTHWISE CONVOLUTIONS

Shayan Jalilpour[1], Gernot R. Müller-Putz[1,2]

[1] Institute of Neural Engineering, Graz University of Technology, Graz, Austria
[2] BioTechMed, Graz, Austria.

E-mail: gernot.mueller@tugraz.at

ABSTRACT: Prior studies have explored the capability of decoding balance perturbations using electroencephalography (EEG) in single-trial classifications. The potential for real-time detection of perturbation-evoked potentials (PEPs) could facilitate the implementation of brain-computer interfaces (BCIs) in everyday assistive systems. Achieving the detection of these potentials in a subject-independent manner is crucial for this advancement. A key step towards this objective is the development of a model capable of identifying balance loss without requiring individual calibration for each subject and enabling online analysis. Deep neural networks have recently achieved significant milestones and have been successfully applied in neural engineering. In this study, we propose a lightweight neural network to assess the viability of single-trial classification of PEPs in a subject-independent manner. Our model was tested on three balance perturbation datasets, demonstrating superior performance in subject-independent classification compared to EEGNet, rLDA, and RBF-SVM classifiers.

INTRODUCTION

Early detection of balance loss offers a promising avenue for preventing falls by enabling brain-computer interfaces (BCIs) as an assistive technology. In recent years, progress has been made in investigating EEG studies related to balance loss [1], [2], [3], [4], [5]. These studies have shown that perturbation-evoked potentials (PEPs) appear in brain signals during balance perturbations [2]. Such event-related potentials (ERPs) comprise different EEG components, including the N1 amplitude -a large negative potential in the fronto-central electrodes, with PEPs primarily characterized by this component. N1 is followed by a positive component, P2, and finally a negative wave called N2. Numerous studies have examined how the brain responds to different balance perturbations and have explored the effects of various stimuli on PEPs. Traditionally, research aimed to uncover the neuroscientific characteristics of PEPs by studying the grand average signals of PEPs [1], [4], [6], [7]. However, few studies have explored the feasibility of incorporating these brain potentials into BCI systems [8], [9]. One of the main steps to achieve this goal is being able to predict balance perturbation in single trials prior to muscle activation to maintain balance. Previously, single trial classification of PEPs was investigated from spontaneous EEG data [9], [10], [11]. In another study, we attempted to classify PEPs in single trials in a simulated asynchronous task and further evaluated the detection of different types of perturbation such as angle and direction by using the brain signals [8], [12].

Given the low signal-to-noise ratio (SNR) in EEG recordings and differences between persons, a classification model trained with EEG data from one person is not transferable to another. This requirement for individual calibration of the BCI system for each user can be both time- and energy- consuming, as it involves collecting sufficient data for every participant. This challenge motivated researchers to develop methods that can mitigate this issue.

Domain adaptation and transfer learning are two techniques developed to address the differences in distribution between target and source domains [13]. However, these methods face challenges that limit their practical application in real-world scenarios [14]. For instance, these techniques rely on the offline adaptation of feature distribution and typically apply adjustments to the pre-built model. To address the challenge of subject-independent classification, we propose a novel neural network designed to detect balance perturbation through subject-independent classification using single trials.

Our model is designed based on neurophysiological principles in a manner that keeps the number of parameters low while simultaneously extracting subject-independent PEP features. We evaluated our model on three EEG balance perturbation datasets: two open-access datasets, and data collected during our two previous studies. We then compared the performance of our model against traditional classification methods, including rLDA and SVM, in addition to well-established neural networks like EEGNet.

MATERIALS AND METHODS

Datasets: We evaluated the models' performance using three datasets. In the first and second datasets, thirty healthy participants were instructed to stand and walk on a treadmill-mounted balance beam [15], [16]. Two electromechanical motors, positioned on the left and right sides of the treadmill, and they were connected to the participants' waists via steel cables. These motors were programmed to rotate a bar attached to the cables

Published by
Verlag der Technischen Universität Graz

10.3217/978-3-99161-014-4-005

by 90 degrees, inducing mediolateral pull perturbations. During both the standing and walking scenarios, each participant experienced 150 perturbations over a session lasting 10 minutes. Brain activity throughout these sessions was recorded using a 128-electrode EEG system (BioSemi ActiveTwo, BioSemi) with a sampling rate of 512 Hz.

The third dataset includes neural recordings from 30 healthy participants, collected through two separate experiments, with each study involving 15 participants [8], [17]. The experimental setup was similar across both studies, where participants were seated in a glider that was tilted in both left and right directions in a simulated aviation scenario. An industrial robot was used to impose these perturbations by tilting the glider at angles of 5 and 10 degrees to simulate balance disruptions. In both experiments, participants completed six blocks, with each block consisting of 40 perturbations in the first study and 50 in the second study, respectively. Brain activity was measured at a sampling rate of 512 Hz with 63 electrodes using an EEGO amplifier (ANT-neuro, Enschede, Netherlands).

To simplify the discussion of dataset-specific findings and analyses, we will adopt specific notations. "Dataset 1" and "Dataset 2" will be used to denote the stand and walking waist perturbation conditions, respectively. "Dataset 3" will represent data from whole-body balance perturbations in simulated aviation scenarios. This notation will ease the discussion of dataset-specific findings and analyses.

Pre-processing: For each dataset, the preprocessing steps were consistent: data was first bandpass-filtered from 0.5 to 30 Hz and subsequently downsampled to 64 Hz. PEP epochs were extracted from the time range of 0 to 1.5 seconds following the perturbation's start. Moreover, rest epochs were segmented before each perturbation onset. Bad EEG channels were detected and eliminated from the rest of analysis. To filter out noise and artifacts, we initially applied Artifact Subspace Reconstruction (ASR) with a threshold value of 30 [18]. This step was followed by the application of independent component analysis (ICA) [19] combined with ICLabel [20] for the removal of eye and muscle artifacts from the EEG data. The processed data were then re-referenced using the common average reference (CAR) technique, and the removed channels were reconstructed through interpolation.

Proposed model: The proposed model begins with a two-dimensional convolutional neural network (CNN) to capture the initial temporal and spatial dependencies of EEG data. This CNN layer uses 15 filters with size of (2,3), followed by batch normalization and the activation function of exponential linear units (ELUs) and a dropout layer with rate of 0.3. Drawing inspiration from the mixed depthwise convolutions introduced by Google researchers [21], the model divides the 15 filters into three tensors, with each tensor comprising 5 filters. Subsequently, depthwise convolutions are applied to the spatial dimension of each tensor individually, with a kernel size denoted by C, which corresponds to the number of channels. Following the extraction of spatial features, the model applies depthwise convolutions to the temporal dimension of the data, employing varying temporal kernel sizes. The sizes of these temporal kernels are 4, 8, and 16, representing temporal durations of 62, 125, and 250 milliseconds, respectively. These temporal kernels were chosen to enable the model to extract the long and short temporal representation of the data. The output features are then subjected to adaptive averaging with a size of 40 and a dropout layer with a rate of 0.65. Afterward, pointwise convolutions with filter size of 5 were applied to the concatenated output from the three tensors, and followed by a dropout layer of 0.5.

All depthwise and pointwise convolutions incorporate batch normalization, the ELU activation function, and a novel attention mechanism known as simAM [22]. Inspired by findings in visual neuroscience, simAM is based on the observation that informative neurons exhibit distinct firing patterns compared to their neighbors, leading to the spatial suppression of surrounding neurons.

In our research, we aim for the model to focus on key electrodes and time periods that are critical for PEP detection. In EEG balance studies, the N1 component appears with high negative amplitude in the frontocentral part of the brain, creating a contrast with other time points and brain areas. This feature allows the simAM mechanism to highlight these crucial periods and electrodes, thereby enhancing PEP identification.

The simAM method compute the importance of each neuron by using the energy function to obtain the linear separability among neurons

$$e_t^* = \frac{4(\beta^2+\lambda)}{(t-\alpha)^2+2\beta^2+2\lambda} \qquad (1)$$

In the above formula, t represents the target neuron, and λ denotes a coefficient with a value of 1e −4.

α and β indicate the mean and variance, respectively, obtained by the formula provided below:

$$\alpha = \frac{1}{M}\sum_{i=1}^{M} x_i \quad (2)$$

$$\beta^2 = \frac{1}{M}\sum_{i=1}^{M}(x_i - \alpha) \quad (3)$$

Published by
Verlag der Technischen Universität Graz

10.3217/978-3-99161-014-4-005

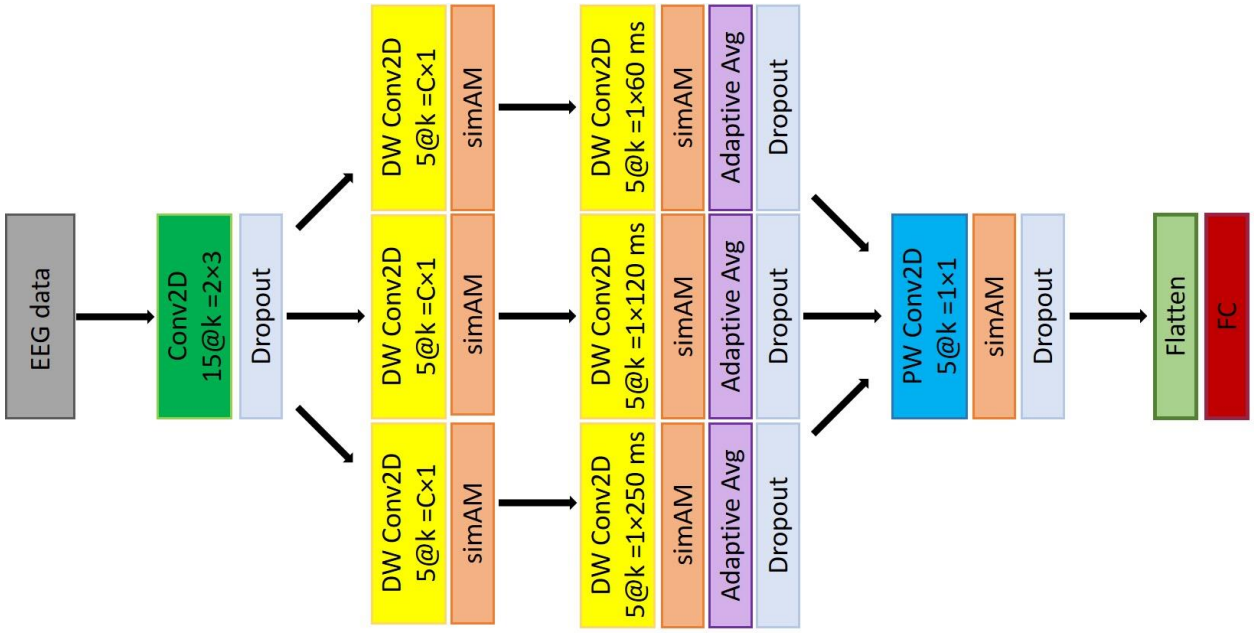

Figure 1. The architecture of proposed model

Where *i* is the index of the neuron, and *M* indicates all the neurons within each filter.
Finally, simAM transforms the input feature map into a new feature of the same size by applying the sigmoid function to the energy function.

$$X = sigmoid\left(\frac{1}{E}\right) \odot X \qquad (4)$$

The last layer of the model consists of a flatten layer and a fully connected layer to generate prediction scores for the PEP and non-PEP classes. The architecture of the model is illustrated in Fig. 1.

Training and Evaluation Approaches: The model was implemented in PyTorch on a GeForce RTX 3080 GPU. AdamW optimizer with a learning rate of 0.001 and weight decay of 1e-2 were used to optimize the parameters. Additionally, we utilized a batch size of 50, and the model was trained for 250 epochs. The evaluation of each model's (classifier's) performance was conducted through the accuracy metric for binary classification tasks.

EXPERIMENTAL RESULTS

ERP Analysis: In Figure 2, we displayed the grand averaged EEG potentials in relation to the onset of perturbations across the three datasets. The analysis revealed that in the first and second datasets, the Perturbation Evoked Potentials (PEPs) consisted of three distinct components: P1, N1, and P2. Notably, the standing condition exhibited higher PEP amplitudes compared to the walking condition. For the third dataset, the PEPs were predominantly characterized by the N1 component located in the brain's central region. These observed differences can be linked to the task designs' variations; specifically, perturbations in the first and second datasets targeted the participants' waist, while the third dataset involved perturbations affecting the entire body. Additionally, the N1 component in the third dataset demonstrated the highest negative amplitude compared to those in the first and second datasets.

Classification: For the first and second dataset, we utilized a leave one subject out approach with 30 participants to assess our model's PEP detection. In this approach, data from one subject served as the test set while data from the remaining 29 subjects constituted the training set. For the third dataset, we employed the recorded data from the first study as the training set and the data collected from the second study as the test set. As a foundation for comparison, we selected shrinkage LDA, RBF-SVM, and EEGNet [23] as baseline models to evaluate the performance of our proposed model. In addition to accuracy, we compared each model's number of trainable parameters. For the sLDA and SVM classifiers, we limited the number of features to 600 using the Fisher algorithm to select the best 600 features. This was done to prevent overfitting, maintaining a feature-to-sample ratio of 1/10. Tab. 1 and 2 shows the obtained accuracy for the standing and walking conditions for 4 models respectively. In the standing condition, it can be seen that neural network models can improve the accuracy substantially in comparison with traditional machine learning algorithms such as sLDA and SVM. The model exhibited superior performance compared to sLDA and SVM, with improvements of 9.2% and 8%, respectively. The proposed model achieved the highest performance, with an average accuracy of 86.9%, and it outperformed the EEGNet model by achieving a 1.6% increase in accuracy while having 16% fewer parameters.

Published by
Verlag der Technischen Universität Graz

10.3217/978-3-99161-014-4-005

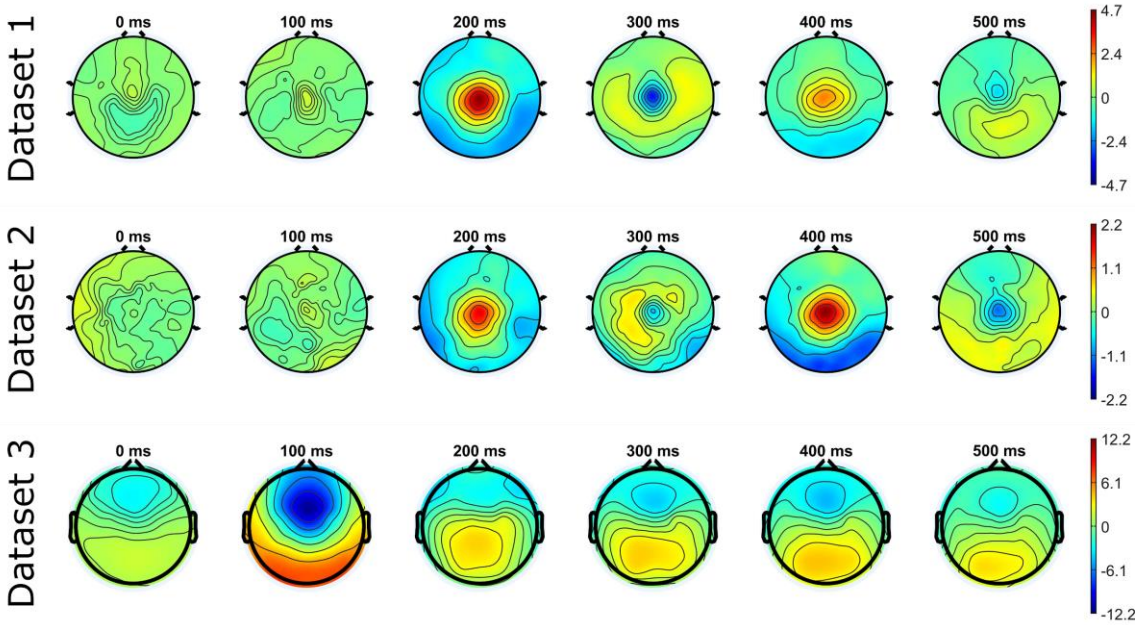

Figure 2. The scalp topography of three datasets in the time range of 0, 100, 200, 300, 400 and 500 ms. For improved visualization, we adjusted the amplitude scales differently for each dataset. The scales range from [-4.7, 4.7], [-2.2, 2.2], to [-12.2, 12.2] microvolts.

Table 1: Results of Dataset 1 (standing condition)

Model	Accuracy (%)	#of parameters
sLDA	77.7	600
SVM	78.9	600
EEGNet	85.3	3248
Our model	86.9	2727

Tab. 2 presents the average subject-independent classification accuracy for the walking condition, noting that due to the smaller PEP amplitude compared to the standing condition, the accuracy in detection of perturbation was lower than the standing condition. For this dataset as well, the proposed model led in performance, attaining an accuracy of 71.8%. EEGNet came in second with a 70% accuracy rate. Following these, SVM and LDA demonstrated accuracies of 66.7% and 65.3%, respectively.

Table 2: Results of Dataset 2 (walking condition)

Model	Accuracy (%)	#of parameters
sLDA	65.3	600
SVM	66.7	600
EEGNet	70	3248
Our model	71.8	2727

Lastly, the model's performance was assessed on the third dataset, which involved participants experiencing balance perturbations in a simulated cockpit scenario. Our model demonstrated superior performance compared to other models. Within neural networks, our model achieved 3.2% higher accuracy than EEGNet while maintaining 20% fewer parameters. Additionally, SVM showed comparable performance to the neural network models, with only 4% difference in accuracy.

Table 3: Results of Dataset 3 (whole body perturbation)

Model	Accuracy (%)	#of parameters
sLDA	87.8	600
SVM	92.4	600
EEGNet	92.8	2208
Our model	96	1752

DISCUSSION

In this research, we investigated the potential of detecting PEPs in a subject-independent manner through EEG single trials, by employing a lightweight CNN-based model. Our approach initially involves extracting spatio-temporal patterns from the data, followed by the implementation of temporal mixed depthwise convolutions using three distinct temporal kernel sizes to accommodate the variability of ERP durations. Additionally, we incorporated a novel attention mechanism, simAM, designed to focus on discriminative features. This attention mechanism is unique in its ability to introduce 3D weights into the model without increasing its parameter count, thereby maintaining a low parameter structure for the model. To assess our model's efficacy, we applied it to three balance perturbation datasets and compared its performance against traditional models like sLDA and SVM, as well as advanced neural networks such as EEGNet. Our findings indicate that

Published by
Verlag der Technischen Universität Graz

10.3217/978-3-99161-014-4-005

neural networks surpass traditional machine learning methods in subject-independent classification across all datasets. Moreover, our model achieved accuracy improvements over EEGNet by 1.3%, 1.8%, and 3.2% for the first, second, and third datasets, respectively. Future endeavors will focus on evaluating our model across additional ERP datasets, also subsequent research will aim at enhancing the model's capability to extract complex spatial patterns of the data.

CONCLUSION

We introduced a novel CNN model that utilizes mixed depthwise convolutions and the simAM attention module to enhance the detection of PEPs from spontaneous EEG data. The efficacy of this model was evaluated across three distinct datasets and its performance was benchmarked against both traditional machine learning techniques and advanced neural networks. Our findings demonstrate that our model achieved the highest accuracy rates when compared with the other models examined.

REFERENCES

[1] V. Dietz, J. Quintern, W. Berger, and E. Schenck, "Cerebral potentials and leg muscle e.m.g. responses associated with stance perturbation," *Exp. Brain Res.*, vol. 57, no. 2, Jan. 1985, doi: 10.1007/BF00236540.

[2] J. P. Varghese, R. E. McIlroy, and M. Barnett-Cowan, "Perturbation-evoked potentials: Significance and application in balance control research," *Neurosci. Biobehav. Rev.*, vol. 83, pp. 267–280, Dec. 2017, doi: 10.1016/j.neubiorev.2017.10.022.

[3] A. L. Adkin, A. D. Campbell, R. Chua, and M. G. Carpenter, "The influence of postural threat on the cortical response to unpredictable and predictable postural perturbations," *Neurosci. Lett.*, vol. 435, no. 2, pp. 120–125, Apr. 2008, doi: 10.1016/j.neulet.2008.02.018.

[4] A. R. Sipp, J. T. Gwin, S. Makeig, and D. P. Ferris, "Loss of balance during balance beam walking elicits a multifocal theta band electrocortical response," *J. Neurophysiol.*, vol. 110, no. 9, pp. 2050–2060, Nov. 2013, doi: 10.1152/jn.00744.2012.

[5] S. M. Peterson and D. P. Ferris, "Group-level cortical and muscular connectivity during perturbations to walking and standing balance," *NeuroImage*, vol. 198, pp. 93–103, Sep. 2019, doi: 10.1016/j.neuroimage.2019.05.038.

[6] R. Goel, S. Nakagome, N. Rao, W. H. Paloski, J. L. Contreras-Vidal, and P. J. Parikh, "Fronto-Parietal Brain Areas Contribute to the Online Control of Posture during a Continuous Balance Task," *Neuroscience*, vol. 413, pp. 135–153, Aug. 2019, doi: 10.1016/j.neuroscience.2019.05.063.

[7] R. Goel, R. A. Ozdemir, S. Nakagome, J. L. Contreras-Vidal, W. H. Paloski, and P. J. Parikh, "Effects of speed and direction of perturbation on electroencephalographic and balance responses," *Exp. Brain Res.*, vol. 236, no. 7, pp. 2073–2083, Jul. 2018, doi: 10.1007/s00221-018-5284-5.

[8] S. Jalilpour and G. Müller-Putz, "Toward passive BCI: asynchronous decoding of neural responses to direction- and angle-specific perturbations during a simulated cockpit scenario," *Sci. Rep.*, vol. 12, no. 1, p. 6802, Apr. 2022, doi: 10.1038/s41598-022-10906-5.

[9] J. C. Ditz, A. Schwarz, and G. R. Müller-Putz, "Perturbation-evoked potentials can be classified from single-trial EEG," *J. Neural Eng.*, vol. 17, no. 3, p. 036008, Jun. 2020, doi: 10.1088/1741-2552/ab89fb.

[10] A. S. Ravindran *et al.*, "Interpretable Deep Learning Models for Single Trial Prediction of Balance Loss," in *2020 IEEE International Conference on Systems, Man, and Cybernetics (SMC)*, Toronto, ON, Canada: IEEE, Oct. 2020, pp. 268–273. doi: 10.1109/SMC42975.2020.9283206.

[11] A. Sujatha Ravindran, C. A. Malaya, I. John, G. E. Francisco, C. Layne, and J. L. Contreras-Vidal, "Decoding neural activity preceding balance loss during standing with a lower-limb exoskeleton using an interpretable deep learning model," *J. Neural Eng.*, vol. 19, no. 3, p. 036015, Jun. 2022, doi: 10.1088/1741-2552/ac6ca9.

[12] S. Jalilpour and G. R. Muller-Putz, "Direction decoding of physical and visual perturbations from EEG," in *2022 IEEE International Conference on Metrology for Extended Reality, Artificial Intelligence and Neural Engineering (MetroXRAINE)*, Rome, Italy: IEEE, Oct. 2022, pp. 427–431. doi: 10.1109/MetroXRAINE54828.2022.9967637.

[13] Z. Wan, R. Yang, M. Huang, N. Zeng, and X. Liu, "A review on transfer learning in EEG signal analysis," *Neurocomputing*, vol. 421, pp. 1–14, Jan. 2021, doi: 10.1016/j.neucom.2020.09.017.

[14] F. Lotte *et al.*, "A review of classification algorithms for EEG-based brain–computer interfaces: a 10 year update," *J. Neural Eng.*, vol. 15, no. 3, p. 031005, Jun. 2018, doi: 10.1088/1741-2552/aab2f2.

[15] S. M. Peterson and D. P. Ferris, "Human electrocortical, electromyographical, ocular, and kinematic data during perturbed walking and standing," *Data Brief*, vol. 39, p. 107635, Dec. 2021, doi: 10.1016/j.dib.2021.107635.

[16] S. M. Peterson and D. P. Ferris, "Differentiation in Theta and Beta Electrocortical Activity between Visual and Physical Perturbations to Walking and Standing Balance," *eneuro*, vol. 5, no. 4, p. ENEURO.0207-18.2018, Jul. 2018, doi: 10.1523/ENEURO.0207-18.2018.

[17] S. Jalilpour and G. Müller-Putz, "Balance

Published by
Verlag der Technischen Universität Graz

10.3217/978-3-99161-014-4-005

perturbation and error processing elicit distinct brain dynamics," *J. Neural Eng.*, vol. 20, no. 2, p. 026026, Apr. 2023, doi: 10.1088/1741-2552/acc486.

[18] T. Mullen *et al.*, "Real-time modeling and 3D visualization of source dynamics and connectivity using wearable EEG," in *2013 35th Annual International Conference of the IEEE Engineering in Medicine and Biology Society (EMBC)*, Osaka: IEEE, Jul. 2013, pp. 2184–2187. doi: 10.1109/EMBC.2013.6609968.

[19] S. Makeig, A. Bell, T.-P. Jung, and T. J. Sejnowski, "Independent Component Analysis of Electroencephalographic Data," in *Advances in Neural Information Processing Systems*, D. Touretzky, M. C. Mozer, and M. Hasselmo, Eds., MIT Press, 1995. [Online]. Available: https://proceedings.neurips.cc/paper_files/paper/1995/file/754dda4b1ba34c6fa89716b85d68532b-Paper.pdf

[20] L. Pion-Tonachini, K. Kreutz-Delgado, and S. Makeig, "ICLabel: An automated electroencephalographic independent component classifier, dataset, and website," *NeuroImage*, vol. 198, pp. 181–197, Sep. 2019, doi: 10.1016/j.neuroimage.2019.05.026.

[21] M. Tan and Q. V. Le, "MixConv: Mixed Depthwise Convolutional Kernels," 2019, doi: 10.48550/ARXIV.1907.09595.

[22] L. Yang, R.-Y. Zhang, L. Li, and X. Xie, "SimAM: A Simple, Parameter-Free Attention Module for Convolutional Neural Networks".

[23] V. J. Lawhern, A. J. Solon, N. R. Waytowich, S. M. Gordon, C. P. Hung, and B. J. Lance, "EEGNet: a compact convolutional neural network for EEG-based brain–computer interfaces," *J. Neural Eng.*, vol. 15, no. 5, p. 056013, Oct. 2018, doi: 10.1088/1741-2552/aace8c.

Published by
Verlag der Technischen Universität Graz